Pharmaceutical Research, Vol. 27, No. 1, January 2010 (© 2009)
DOI: 10.1007/s11095-009-0004-2

Research Paper

Factors Affecting the Stability of Nanoemulsions—Use of Artificial Neural Networks

Amir Amani,[1,2,4] Peter York,[1] Henry Chrystyn,[3] and Brian J. Clark[1]

Received July 25 2009; accepted October 26 2009; published online November 12, 2009

Purpose. The aim of this study was to identify the dominant factors affecting the stability of nanoemulsions, using artificial neural networks (ANNs).
Methods. A nanoemulsion preparation of budesonide containing polysorbate 80, ethanol, medium chain triglycerides and saline solution was designed, and the particle size of samples with various compositions, prepared using different rates and amounts of applied ultrasonic energy, was measured 30 min and 30 days after preparation. Using ANNs, data were modelled and assessed. The derived predictive model was validated statistically and then used to determine the effect of different formulation and processing input variables on particle size growth of the nanoemulsion preparation as an indicator of the preparation stability.
Results. The results indicated that the data can be satisfactorily modelled using ANNs, while showing a high degree of complexity between the dominant factors affecting the stability of the preparation.
Conclusion. The total amount of applied energy and concentration of ethanol were found to be the dominant factors controlling the particle size growth.

KEY WORDS: artificial neural networks; budesonide; microemulsion; nanoemulsion; particle size; stability.

INTRODUCTION

Micro- and nanoemulsion formulations have shown potential for the delivery of poorly water soluble drugs. Ease of preparation, increased bioavailability and potential for sustained release of drugs are features of these formulations which have attracted the attention of researchers in the pharmaceutical industries and academia (1–3). However, literature reports have indicated a wide range of physical stability for such preparations, with examples being physically stable from a few days to more than 2 years (1).

A possible mechanism for the stability in micro- and nanoemulsions was first proposed by Ruckenstein and Chi (4). They proposed that the change in free energy of formation of these preparations is affected by three factors: changes in interfacial free energy, energy of interactions between the droplets and the effect made by entropy of dispersion. It was proposed that whilst the energy of interactions between the droplets was negligible, the interfacial free energy could be zero or even negative if the interfacial tension lies between 10-2-10-13 mN/m (4). Instability then occurs due to the Ostwald ripening effect, with coalescence of particles leading to increase in the size of nanoparticles and thereby destabilization of the nanodroplets with subsequent sediment of particles (5,6).

Addition of salt and/or other formulation additives, as well as the temperature and pressure, are factors which can affect the physical stability of micro- and nanoemulsions (7). The surface charge (Zeta potential) of the particles (8), molecular structure of co-surfactant, ratio of hydrophilic to hydrophobic components (9), ratio of co-surfactants and surfactant(s) to co-surfactant(s) (10) and molecular structure of the oil (11) are also reported to have a role in determining the stability of the these formulations. However, reported work detailing the relative importance of these factors as well as examination of the interactions between the experimentally measured variables has not provided a comprehensive study of the different formulation parameters controlling the stability of the preparation. This is thought to be due to the complexity of the formulations and preparation processes involved.

In recent years, Artificial Neural Networks (ANNs) have been widely used to examine complex, multivariable processes when classical statistical techniques fail to model and/or quantify the relationships between variables and/or outputs (12,13). ANNs work on the basis of linking neurons to generate an output based on the associated weights (showing the importance) of input(s) by computing the weighted sum of all inputs. Usually, the neurons are identical and form a three-layer structure input layer to take the input variables, hidden layer(s) to compute the relation between variables and output and an output layer to report the results (14).

[1] Institute of Pharmaceutical Innovation, School of Pharmacy, University of Bradford, BD7 1DP, Bradford, UK.
[2] Department of Medical Nanotechnology, School of Advanced Medical Technologies, Tehran University of Medical Sciences, Tehran, 1417614411, Iran.
[3] School of Applied Sciences, University of Huddersfield, HD1 3DH, Huddersfield, UK.
[4] To whom correspondence should be addressed. (e-mail: aamani@sina.tums.ac.ir)

In previous work (15), we reported the relative influence of five different formulation and processing variables on the particle size of the nanoemulsions produced—defined here as any emulsion particles below 100 nm (3). Total energy applied to the preparation was found to be the most important factor (15). The aim of this study is to use ANNs to identify possible hidden factors which also influence the growth of particle size in prepared nanoemulsions, thus providing insight into the stability of such preparations.

MATERIALS AND METHODS

Materials

Medium chain triglyceride (MCT), Crodamol GTCC, was a gift from Croda (UK). Budesonide (Pharm. Eur.) was from Industriale Chimica s.r.l. (Italy). Pharmaceutical grade polysorbate 80 was purchased from Fluka (Switzerland). All other chemicals were of analytical grade and purchased from Sigma-Aldrich (USA).

Preparation of Samples and Particle Size Measurement

Nanoemulsion samples (20 ml) containing polysorbate 80, MCT, ethanol, budesonide in saline solution were prepared using a VCX500 probe sonicator (Sonics and Materials, USA) following the method described previously (15). Samples were then filtered through 0.2 μm syringe filters, and the particle size was measured 30 min after preparation using a Zetasizer Nano (Malvern, UK). The mean size (Z-average size) of five replicates at 25°C based on Photon Correlation Spectroscopy (PCS) was taken as the particle size. No dilution was performed on the samples prior to measurement. Dispersant viscosity was set as 0.8872cP at 25°C (15).

Samples were then stored in sealed, sterile cylindrical containers with the internal diameter of 2.3 cm at 30°C, and a second measurement was performed after 30 days storage. The ratio of growth (i.e. $\frac{particle\ size\ after\ 30\ days}{particle\ size\ after\ 30\ minutes}$) was considered as an indication of the physical stability of the various samples.

Data Mining Tool

INForm v3.5 (Intelligensys, UK), a commercial ANN employed in this study, was used to model the non-linear and complex relations between inputs and outputs. Results from these analyses are illustrated as 3D graphs, rather than statistical models, which can be used to characterise interactions between inputs and output.

Data Set

Using INForm v3.5, the available data are often randomly divided into three sets: the training set, test set and validation set. In this case, the network is trained by the training data set, the test set is used to stop the learning process and the ability of trained network is assessed using a set of unseen data (validation data) (16).

The preparation process for the nanoemulsion involved seven ingredients/processing conditions variables for each experiment: percentage of polysorbate 80 (weight %), ethanol (weight %) and oil (weight %), budesonide dissolved in 20 ml of the preparation (mg/20 ml), saline normality (N), total energy applied (J) and rate of energy applied (RAE) (J/min) to the preparation. As described previously (15), the percentages of polysorbate 80 and oil were fixed at 10% (weight %) and 1% (weight %), respectively, to represent the realistic situation while formulating nanoemulsions for pharmaceutical purposes. As a result, five input variables were considered in the training stage of data mining and varied randomly in each experiment. The particle size growth ratio obtained was the single output.

The growth in particle size of 35 samples (each of 20 ml final volume in sealed containers), all having a fixed ratio of surfactant/oil (10:1), was investigated over 30 days for samples stored at 30°C. The particle size growth ratio was calculated with the most physically stable preparation expected to have the closest particle growth ratio to unity.

To prevent computer-based overtraining during the training stage, two approaches were employed. The maximum number of iterations was set to 1000 (i.e. the default value). Furthermore, three individual data records (i.e. 10% of the data set as recommended by the software) was randomly taken out of the training process as test data and used to avoid overtraining (i.e. "test data"). If the network is becoming overtrained, the correlation coefficient obtained for the test data starts (see Eq. 1) to decrease and the training process stops. Therefore, 32 of the individual sets of experimental results were used as "training data" to set up the cause-effect relationships between the inputs and the output. Additionally, 14 supplementary experiments were performed, and the results were excluded from training to be used as unseen or "validation data." Subsequent to training, the validation data were employed to evaluate the predictive ability and quality of the generated model. Tables I and II list the values of input variables that were prepared and subsequently examined.

Training Parameters

Details of learning algorithms and training parameters interrogated to optimise the network structure have been described previously (16,17). Subsequent to training the network, using the parameters listed in Table III, the predicted value of particle growth ratios was determined from the derived model, and the quality of training and the predictability of the models were validated using the correlation coefficient R-square (R^2) for training, test and validation data.

$$R^2 = 1 - \frac{\sum_{i=1}^{n} \left(y_i - \hat{y}_i\right)^2}{\sum_{i=1}^{n} \left(y_i - \bar{y}_i\right)^2} \quad (1)$$

where $\bar{y}$ is the mean of dependent variable, and $\hat{y}$ is the predicted value from the model. A quality ANN model should have an acceptable R^2 for all training, test and validation data.

RESULTS AND DISCUSSION

After modelling the data using the ANN, the best predictive model resulted in R^2 values of 0.95, 0.89 and 0.82 for the training, test and validation data, respectively. These values indicate a good-quality trained model. The observed

Table I. Formulation and processing conditions (i.e. the test and training data set, used in ANNs modelling, last three individual experiments represent the "test data")

Input parameters						Output parameter		
Sample no.	Ethanol (weight %)	Budesonide (mg/20 ml)	Total energy applied (J)	Saline (N)	RAE (J/min)	Particle size (30 min) (nm)	Particle size (30 days) (nm)	Particle growth ratio
1	1.1	30.0	3540	0.6	1295	10.8	13.0	1.2
2	1.8	20.6	2000	0.4	1714	16.9	82.8	4.9
3	1.0	10.1	2900	1	635	17.3	55.4	3.2
4	1.7	21.9	2650	1.1	1626	18.5	44.4	2.4
5	1.9	23.3	1700	1.8	911	18.0	45.0	2.5
6	1.0	30.0	2050	0.6	665	23.8	47.6	2.0
7	2.0	30.0	2050	0.6	661	24.7	101.3	4.1
8	2.0	0.0	2050	0.6	661	18.7	56.1	3.0
9	2.0	29.8	2050	0.6	647	22.1	44.2	2.0
10	1.1	30.0	3540	0.6	1249	11.3	13.6	1.2
11	1.3	28.6	2050	0.3	1255	19.2	84.5	4.4
12	1.0	29.8	3000	0.6	1241	11.5	15.0	1.3
13	1.0	30.1	3000	0.6	1935	44.0	74.8	1.7
14	1.0	29.8	3000	0.6	1364	16.2	24.3	1.5
15	1.0	30.0	3000	0.6	1241	11.5	23.0	2.0
16	1.0	30.0	3000	0.6	1268	14.7	20.6	1.4
17	3.0	25.4	6590	0.8	665	11.3	13.6	1.2
18	2.3	26.8	5045	0.5	1125	11.4	18.2	1.6
19	2.8	20.4	2250	0.4	912	19.6	131.3	6.7
20	2.4	22.5	650	1.2	1054	15.0	39.0	2.6
21	2.1	28.0	4560	1.2	837	11.7	12.9	1.1
22	2.6	28.7	1790	0.3	1513	24.8	119.0	4.8
23	2.2	29.9	2840	0.9	658	19.5	29.3	1.5
24	1.6	23.9	3850	0.5	1582	11.6	13.9	1.2
25	2.0	20.4	1315	0.7	1384	18.6	35.3	1.9
26	1.1	16.0	4417	0.8	1031	11.0	12.1	1.1
27	2.6	28.1	5735	0.9	1955	12.1	16.9	1.4
28	1.5	17.1	2743	0.3	735	22.0	46.2	2.1
29	2.6	13.0	2415	0.3	805	22.8	177.8	7.8
30	2.0	20.9	1450	1.0	1279	21.4	79.2	3.7
31	1.6	22.3	4340	0.8	1033	11.7	12.9	1.1
32	2.0	25.5	5540	[a]	906	11.1	32.2	2.9
33	2.4	19.1	2500	0.4	1014	22.8	187.0	8.2
34	1.0	30.0	5300	0.5	967	11.1	12.2	1.1
35	1.0	23.3	1089	1.4	895	16.2	27.5	1.7

[a] missing data

and predicted particle growth ratios for the training, test and validation data are listed in Tables IV, V and VI, respectively, and Fig. 1 shows a plot of predicted and observed nanoemulsion particle size growth ratio for the 14 individual sets of validation experimental data.

This generated model was then employed to study the effects of the different input variables on the particle size growth of the nanoemulsions.

The results obtained revealed a high degree of complexity when attempting to identify the dominating factors controlling the increase in nanoemulsion particle size when compared to the analysis of the influence of input parameters on the initial particle size (15). While a sensitivity analysis approach can be used to provide ranking of input variables, in this study a systematic approach was followed. Briefly, this approach involves investigating the effect of variation of two specific input variables on the output, visualized by 3D graphs generated by the model, while the remaining input variables are fixed at three specific value—namely a low, mid-range and high value (15,18). In following this method, the results were divided into three groups: zero, medium, and high concentration of budesonide. For each of these three groups, 3D plots of total energy-ethanol-size growth at a mid-range value of saline and RAE were considered. Each plot was also accompanied by four additional complementary plots to illustrate the effect of low and high values of saline and RAE on the particle size growth.

Zero Concentration of Budesonide in the Formulation

Figure 2a shows 3D plots of size-growth ratio against concentration of ethanol and the total applied energy at mid-range values of saline concentration and RAE. This figure is accompanied by four additional plots (Fig. 2b–e) of high and low values of saline and RAE. Employing this method, the obtained model can be "visualized" using generated 3D

Table II. Validation data set used to validate the generated model

	Input parameters					Output parameter		
Sample no.	Ethanol (weight %)	Budesonide (mg/20 ml)	Total energy applied (J)	Saline (N)	RAE (J/min)	Particle size (30 min) (nm)	Particle size (30 days) (nm)	Particle growth ratio
36	2.0	30.0	2050	0.6	631	21.6	67.0	3.1
37	1.3	29.7	4650	1.5	1197	11.1	12.2	1.1
38	2.0	0.0	2090	0.6	643	19.4	77.6	4.0
39	1.3	29.7	4650	1.5	1368	11.1	12.2	1.1
40	1.0	30.1	3000	0.6	629	14.4	18.7	1.3
41	1.0	30.0	3000	0.6	1440	19.0	39.9	2.1
42	2.5	30.0	1050	0.3	1575	18.2	67.3	3.7
43	2.9	20.0	3150	0.6	1370	16.2	42.1	2.6
44	2.5	21.1	3610	0.6	926	11.7	17.6	1.5
45	1.5	25.2	2450	0.7	1771	20.0	38.0	1.9
46	2.3	21.5	1990	0.5	1405	20.4	100.0	4.9
47	1.5	24.5	5425	0.7	779	11.4	12.5	1.1
48	2.6	29.5	4093	1.0	1266	12.3	14.8	1.2
49	1.7	27.0	3719	0.9	1344	11.6	12.8	1.1

graphs, leading to easier interpretation of the results as explained previously (15,18). By comparing the series of 3D plots, the rules describing the relationships between input and output parameters can be identified.

From Fig. 2, the plots demonstrate that particle size growth is minimal at the highest values of total applied energy and lowest percentages of ethanol (see the region represented by Number 1 in Fig. 2a–e). Also, on increasing the salinity of dispersant, the overall growth decreases (i.e. the plots representing low *vs*. high values of saline in Fig. 2b and c *vs*. Fig. 2e and d). The peak in particle growth ratio, observed in the region of 2500 J applied energy (see the line represented by Number 2 in Fig. 2a–e) is an interesting factor. This peak appears to represent a transitional state (TS) in which the growth ratio increases. This maximum could be related to the TS in particle size 3D plots previously reported (15) and is thought to be associated with rearrangement of the component molecules in the nanoemulsion structure.

Figure 2d and e also show that the concentration of saline influences the stabilization of the particles, with higher values leading to increased physical stability. This is attributed to changes in intra- and inter-particle interactions which are modified by addition of saline ions. It is also apparent that, in general, the RAE does not affect the particle growth ratio (i.e. the plots representing low *vs*. high values of RAE in Fig. 2b and d *vs*. Fig. 2c and e). The exception is at high values of RAE where a maximum is observed at high values of ethanol and total applied energy (see the region represented by Number 3 in Fig. 2c and e). One possible explanation is that the degree of complexity of the mechanisms controlling the physical stability of the nanoemulsion is increasing at higher energy rates (i.e. the nanoemulsion components restructure again at high energy rates), which leads to a second maximum in the growth ratio in addition to the peak in the TS region. This peak is apparent in high RAE and low salinity values (see Fig. 2c and e). However, at high concentration of saline (i.e. Fig. 2e), this peak has been largely masked by the effect of the concentration of saline which acts in favour of stabilizing the nanoemulsion particles.

Medium Concentration of Budesonide in the Formulation

The second step in interpreting the 3D graphs is to assess the input-output relations in mid-range values of the fixed

Table III. The training parameters set with INForm v3.5

Network structure	No. of hidden layers	1
	No. of nodes in hidden layer	5
Backpropagation type		Angle Driven Learning
Backpropagation parameters	Momentum factor	0.8
	Learning rate	0.7
Targets	Maximum iterations	1000
	MS error	0.0001
	Random seed	10000
Smart stop	Minimum iterations	20
	Test error weighting	0.1
	Iteration overshoot	200
	Auto weight	On
	Smart stop enabled	On
Transfer function	Output	Asymmetric Sigmoid
	Hidden layer	Asymmetric Sigmoid

Table IV. The observed and predicted particle growth ratio for training data

Sample no.	Observed particle growth ratio[a]	Predicted particle growth ratio[b]
1	1.2	1.1
2	4.9	4.8
3	3.2	2.9
4	2.4	2.7
5	2.5	2.5
6	2.0	2.1
7	4.1	3.2
8	3.0	3.0
9	2.0	2.9
10	1.2	1.1
11	4.4	4.4
12	1.3	1.4
13	1.7	1.8
14	1.5	1.4
15	2.0	1.3
16	1.4	1.3
17	1.2	1.2
18	1.6	1.6
19	6.7	6.6
20	2.6	3.0
21	1.1	1.1
22	4.8	4.8
23	1.5	1.7
24	1.2	1.3
25	1.9	2.5
26	1.1	1.1
27	1.4	1.4
28	2.1	2.3
29	7.8	7.7
30	3.7	2.6
31	1.1	1.1

[a] The particle size growth ratio calculated in Table I
[b] The predicted particle size growth ratio, using ANNs modelling

input parameter. Figure 3 shows data for the nanoemulsion preparation containing 15 mg/20 ml concentration of budesonide. From the trends discussed in "Zero Concentration of Budesonide in the Formula" (i.e. zero budesonide), three distinct observations describe effects at medium concentrations of budesonide: 1) the higher the energy and the lower the percentage of ethanol, the smaller the size growth ratio (i.e. Number 1 in Fig. 3a–e), 2) a TS exists in all Figures (i.e. Number 2 in Fig. 3a–e), and 3) a second maximum is observed at high values of RAE at low concentration of saline (i.e. Number 3 in Fig. 3c).

Table V. The observed and predicted growth ratio for test data

Sample no.	Observed particle growth ratio[a]	Predicted particle growth ratio[b]
32	8.2	6.47
33	1.1	1.21
34	1.7	1.08

[a] The particle size growth ratio calculated in Table I
[b] The predicted particle size growth ratio, using ANNs modelling

Table VI. The observed and predicted growth for validation data

Sample no.	Observed particle growth ratio[a]	Predicted particle growth ratio[b]
36	3.1	2.8
37	1.1	1.1
38	4.0	3.1
39	1.1	1.1
40	1.3	1.9
41	2.1	1.4
42	3.7	3.7
43	2.6	1.8
44	1.5	1.4
45	1.9	2.9
46	4.9	4.5
47	1.1	1.3
48	1.2	1.3
49	1.1	1.1

[a] The particle size growth ratio calculated in Table II
[b] The predicted particle size growth ratio, using ANNs modelling

The effect of saline on the growth (i.e. the plots representing low *vs*. high values of saline in Fig. 3) shows a complex pattern in the presence of budesonide at medium concentrations. The profiles in Fig. 3b and c compared to Fig. 3d and e suggest that in medium concentrations of budesonide, saline does not influence the particle size growth. This effect will be considered later.

High Concentration of Budesonide in the Formulation

Figure 4a–e shows the 3D plots for high concentrations of budesonide. As observed for zero and medium concentrations, the results indicate that the two major factors dominating low values of growth ratio are reducing ethanol concentration and increasing total applied energy. However, on comparing the plots in Figs. 2, 3 and 4, it can be seen that in the region of high concentration of ethanol and low applied energy (i.e. absence of the two major controlling factors), incorporation of budesonide in the nanoemulsion particles counteracts the effect of saline. For systems without budeso-

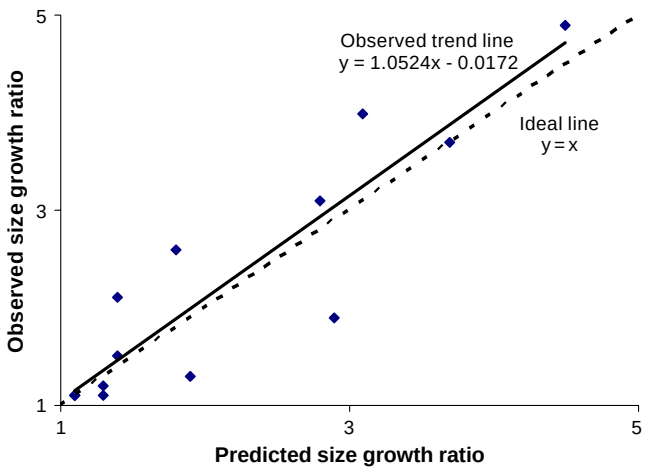

Fig. 1. Validation agreement plot of ANN for validation data for particle size growth.

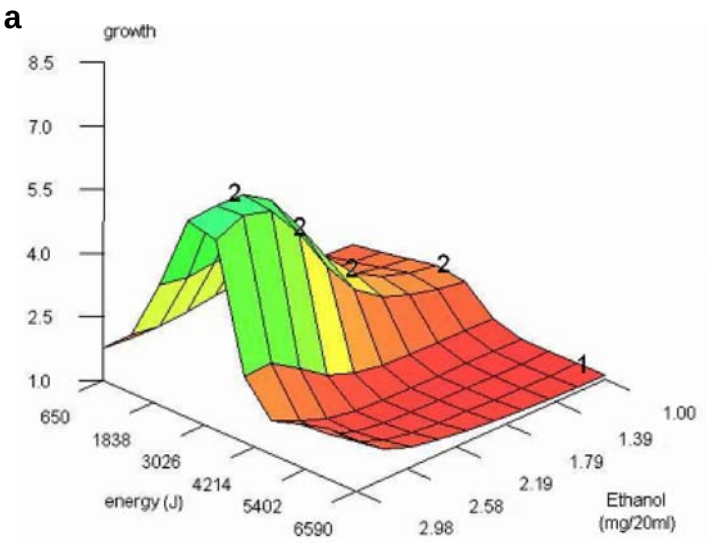

RAE	Saline		RAE	Saline	
Low	Low	b	High	Low	c
Low	High	d	High	High	e

Fig. 2. **a** 3D plot of particle size growth predicted by the ANN model for total applied energy and ethanol concentration at fixed mid-range values of 1.0 (N) and 1200 (J/min) for saline and RAE, respectively, at zero budesonide in the preparation. **b–e** Four complimentary plots representing high and low values for concentration of saline and RAE inputs at zero budesonide in the preparation. The values for fixed input factors in small plots are saline 0.6 and 1.4 (N) and RAE 915.0 and 1486.0 (J/min), where applicable.

nide (i.e. Fig. 2), it was observed that addition of saline led to increased stability, whilst on increasing the concentration of saline in budesonide-loaded nanoemulsion particles (i.e. Fig. 3d and e *vs* Fig. 3b and c as well as Fig. 4d and e *vs* Fig. 4b and c), the size growth did not decrease and even increased in high concentrations of budesonide. This observation is thought to be due to the fact that budesonide is accommodated in the core of the nanoemulsion particles, which leads to changes in the intra-particle interactions in favour of hydrophobic forces (15). At high concentration of ethanol and low applied energy values, saline ions stabilize the nanoemulsion particles through hydrophilic inter- and intra-particular interactions, which are counteracted by the budesonide molecules, and thus, the increase in concentration of saline does not lead to an overall increase in the stability of the preparation in the presence of the budesonide molecules. The second peak in growth ratio generated due to increasing the RAE in low saline concentrations is also observed in Fig. 4c, although was more pronounced in Figs. 2c and 3c (see Number 3 in Fig. 4c). As discussed earlier, this phenomenon

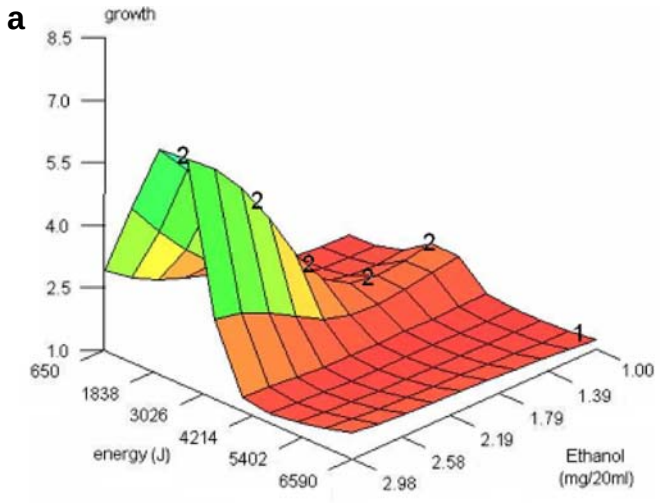

RAE	Saline		RAE	Saline	
Low	Low	b	High	Low	c
Low	High	d	High	High	e

Fig. 3. **a** 3D plot of particle size growth predicted by the ANN model for total applied energy and ethanol concentration at fixed mid-range values of 1.0 (N) and 1200 (J/min) for saline and RAE, respectively, at medium budesonide in the preparation (i.e. 15 mg/20 ml). **b–e** Four complimentary plots representing high and low values for concentration of saline and RAE inputs at medium budesonide in the preparation (i.e. 15 mg/20 ml). The values for fixed input factors in small plots are saline 0.6 and 1.4 (N) and RAE 915.0 and 1486.0 (J/min), where applicable.

could be associated with formation of intra-particle interaction in high concentrations of budesonide.

From the above analyses, the following general rules can be identified for preparing a stable nanoemulsion with minimal particle size growth containing budesonide:

1. Effect of total applied energy: by increasing the total applied energy, the physical stability of the formulation increases. A minimum amount of applied energy (approximately 4500 J for 20 ml preparation) is required for nanoemulsion components (i.e. oil, surfactant and co-surfactant) to be organized into a construct that generates the most stable particle. Also, it is interesting to note that in all 3D figures illustrated in Figs. 2, 3 and 4, a peak at 2500 J applied energy (i.e. medium amounts of energy) is frequently observed which is attributed to a transient displacement of components (i.e. TS).
2. Effect of ethanol percentage: by decreasing the percentage of ethanol from 3% to 1% (w/w) (i.e. from maximum to minimum), the nanoemulsion exhibits greater physical stability. This finding indicates that only a minimum amount of co-surfactant is necessary for the formation and stabilization of the nanoemulsion

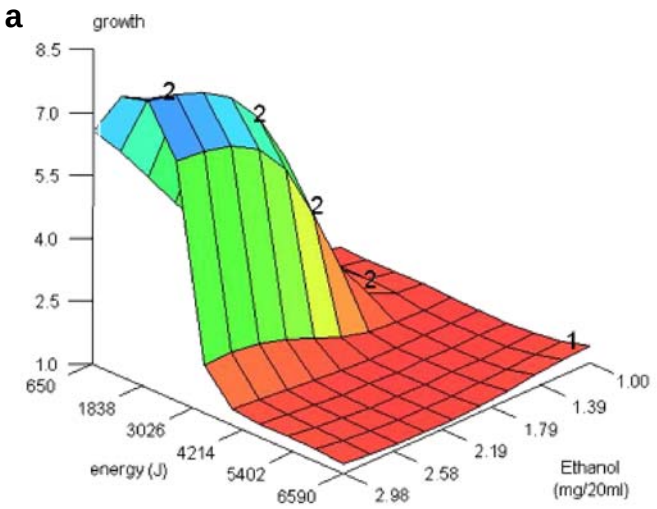

RAE	Saline		RAE	Saline	
Low	Low	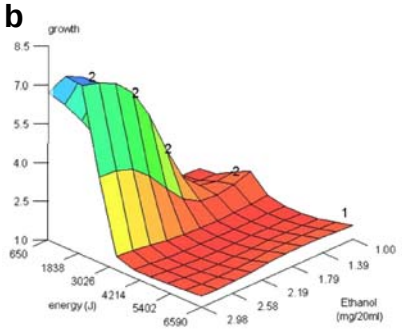	High	Low	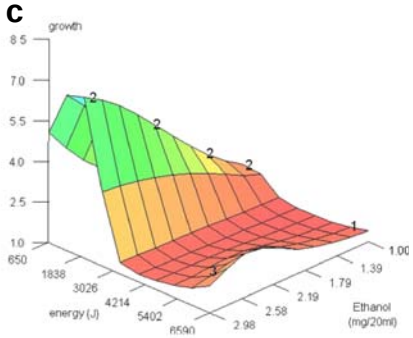
Low	High	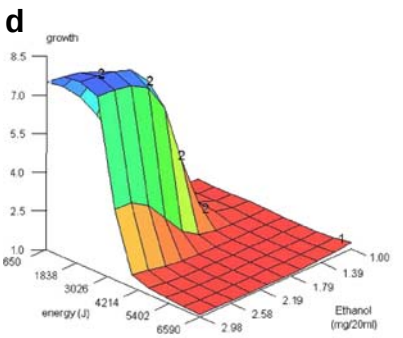	High	High	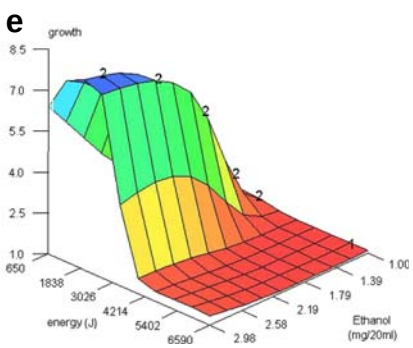

Fig. 4. **a** 3D plot of particle size growth predicted by the ANN model for total applied energy and ethanol concentration at fixed mid-range values of 1.0 (N) and 1200 (J/min) for saline and RAE, respectively, at high concentration of budesonide in the preparation (i.e. 30 mg/20 ml). **b**–**e** Four complimentary plots representing high and low values for concentration of saline and RAE inputs at high concentration of budesonide in the preparation (i.e. 30 mg/20 ml). The values for fixed input factors in small plots are saline 0.6 and 1.4 (N) and RAE 915.0 and 1486.0 (J/min), where applicable.

and the additional amounts of co-surfactant may interact unfavourably with other components of the nanoemulsion leading to reduced physical stability.

3. Effect of saline: saline appears to provide more physically stable nanoemulsion preparations in the absence of the budesonide molecules. The effect of saline on the stability can be explained through changes in intra- and, more specifically, inter-particle interactions.
4. Effect of applied energy rate: high energy rates generally led to the generation of a second peak in the size growth ratio at low levels of saline. This effect is attributed to another rearrangement in the location of the nanoemulsion components.

CONCLUSIONS

The work reported showed the capability of ANNs to identify the primary factors controlling particle size growth in nanoemulsions. From the 3D graphs developed from the model, it was interpreted that the arrangement of the preparation

components plays the key factor in stabilizing the nanoparticles with total applied energy and percentage of ethanol as the critical parameters controlling particle size growth on storage. By increasing the total applied energy to levels above 4500 J and for concentration levels of ethanol at 1% w/w, the most physically stable formulation was obtained. Moreover, it was found that incorporation of budesonide counteracted the effect of saline in stabilizing the nanoparticles.

REFERENCES

1. Tenjarla S. Microemulsions: an overview and pharmaceutical applications. Crit Rev Ther Drug Carrier Syst. 1999;16:461–521.
2. Ghosh PK, Murthy RS. Microemulsions: a potential drug delivery system. Curr Drug Deliv. 2006;3:167–80.
3. Sarker DK. Engineering of nanoemulsions for drug delivery. Curr Drug Deliv. 2005;2:297–310.
4. Ruckenstein E, Chi JC. Stability of microemulsions. J Chem Soc Faraday Transactions. 1975;2(71):1690–707.
5. Debuigne F, Cuisenaire J, Jeunieau L, Masereel B, Nagy JB. Synthesis of nimesulide nanoparticles in the microemulsion epikuron/isopropyl myristate/water/n-butanol (or isopropanol). J Colloid Interface Sci. 2001;243:90–101.
6. Karasulu HY. Microemulsions as novel drug carriers: the formation, stability, applications and toxicity. Expert Opin Drug Deliv. 2008;5:119–35.
7. Paul BK, Moulik SP. Uses and applications of microemulsions. Curr Sci. 2001;80:990–1001.
8. Müller RH, Heinemann S. Fat emulsions for parenteral nutrition. I: Evaluation of microscopic and laser light scattering methods for the determination of the physical stability. Clin Nutr. 1992;11:223–36.
9. von Rybinski W, Guckenbiehl B, Tesmann H. Influence of co-surfactants on microemulsions with alkyl polyglycosides. Colloids Surf A Physicochem Eng Asp. 1998;142:333–42.
10. Wang HJ, Zhichao D. Study on formation of microemulsions with systems containing water, aerosol-AOT and ethyl linoleate. Zhongguo Yaoxue Zazhi. 1998;33:540–3.
11. Eastoe JR, Steytler DC. A study of microemulsion stability. NATO ASI Series, Series C: Mathematical and Physical Sciences. 1990;324:295–301.
12. Bourquin J, Schmidli H, van Hoogevest P, Leuenberger H. Comparison of artificial neural networks (ANN) with classical modelling techniques using different experimental designs and data from a galenical study on a solid dosage form. Eur J Pharm Sci. 1998;6:287–300.
13. Sathe PM, Venitz J. Comparison of neural network and multiple linear regression as dissolution predictors. Drug Dev Ind Pharm. 2003;29:349–55.
14. Rowe RC, Roberts RJ. Intelligent software for product formulation. London: Taylor & Francis; 1998.
15. Amani A, York P, Chrystyn H, Clark BJ, Do DQ. Determination of factors controlling the particle size in nanoemulsions using artificial neural networks. Eur J Pharm Sci. 2008;35:42–51.
16. Intelligensys. Inform manual. Intelligent formulation (2004).
17. Shao Q, Rowe RC, York P. Comparison of neurofuzzy logic and neural networks in modelling experimental data of an immediate release tablet formulation. Eur J Pharm Sci. 2006;28:394–404.
18. Ali HSM, Blagden N, York P, Amani A, Brook T. Artificial neural networks modeling the prednisolone nanoprecipitation in microfluidic reactors. Eur J Pharm Sci. 2009;37:514–22.